



PARP inhibitor olaparib has a potential to increase the effectiveness of electrochemotherapy in *BRCA1* mutated breast cancer in mice

Masa Bosnjak^{a,b,*}, Tanja Jesenko^{a,c}, Bostjan Markelc^{a,d}, Larisa Janzic^c, Maja Cemazar^{a,e}, Gregor Sersa^{a,d,*}

^a Institute of Oncology Ljubljana, Zaloska 2, SI-1000 Ljubljana, Slovenia

^b University of Ljubljana, Faculty of Pharmacy, Askerceva 7, SI – 1000 Ljubljana, Slovenia

^c University of Ljubljana, Faculty of Medicine, Korytkova 2, SI – 1000 Ljubljana, Slovenia

^d University of Ljubljana, Faculty of Health Sciences, Zdravstvena pot 5, SI – 1000 Ljubljana, Slovenia

^e University of Primorska, Faculty of Health Sciences, Polje 42, SI – 6310 Izola, Slovenia

ARTICLE INFO

Article history:

Received 31 December 2020

Received in revised form 22 April 2021

Accepted 23 April 2021

Available online 1 May 2021

Keywords:

Electrochemotherapy

Bleomycin

Cisplatin

Olaparib

Breast cancer

ABSTRACT

Electrochemotherapy (ECT), a local therapy, has different effectiveness among tumor types. In breast cancer, its effectiveness is low; therefore, combined therapies are needed. The aim of our study was to combine ECT with PARP inhibitor olaparib, which could inhibit the repair of bleomycin or cisplatin induced DNA damage and potentiate the effectiveness of ECT. The effects of combined therapy were studied in *BRCA1* mutated (HCC1937) and non-mutated (HCC1143) triple negative breast cancer cell lines. Therapeutic effectiveness was studied in 2D and 3D cell cultures and *in vivo* on subcutaneous HCC1937 tumor model in mice. The underlying mechanism of combined therapy was determined with the evaluation of γ H2AX foci. Combined therapy of ECT with bleomycin and olaparib potentiated the effectiveness of ECT in *BRCA1* mutated HCC1937, but not in non-mutated HCC1143 cells. The combined therapy had a synergistic effect, which was due to the increased number of DNA double strand breaks. Addition of olaparib to ECT with bleomycin *in vivo* in HCC1937 tumor model had only minimal effect, indicating repetitive olaparib treatment would be needed. This study demonstrates that DNA repair inhibiting drugs, like olaparib, have the potential to increase the effectiveness of ECT with bleomycin.

© 2021 The Author(s). Published by Elsevier B.V. This is an open access article under the CC BY-NC-ND license (<http://creativecommons.org/licenses/by-nc-nd/4.0/>).

1. Introduction

Breast cancer is the most frequently diagnosed malignancy and is globally still the leading cause of cancer death in women. Even though this is a highly curable disease in developed countries, approximately 10–15% of all breast cancer patients develop a loco-regional recurrence within 10 years. About 10–20% of breast cancers are negative for estrogen and progesterone receptors, and amplification of *HER2* gene, which means they are triple-negative. Such breast cancer is considered to be more aggressive and have a poorer prognosis, mainly because there are fewer available targeted therapies. Therefore, there is an urge to discover new therapies or combinations of therapies that could benefit triple negative breast cancer patients [1].

Metastatic breast cancer patients are unlikely to be cured of their disease and the main goal of the treatment is to palliate the

symptoms, prolong survival, and maintain quality of life [2,3]. For such patients presented with skin metastases one of the treatment options is also electrochemotherapy (ECT) [4]. ECT is a local tumor therapy, based on a physical delivery method, electroporation. It facilitates the entrance of cytotoxic drugs to cells and tissues [5,6]. In ECT, bleomycin and cisplatin are two of the most commonly used cytotoxic drugs. Main target of ECT with bleomycin or cisplatin is DNA, as both exert their cytotoxic effect through DNA damage, causing DNA breaks or adducts, respectively. Bleomycin induces single and double DNA strand breaks [7]. Cisplatin interferes with DNA replication; it forms inter- and intrastrand DNA adducts and thus stall replication forks during S-phase [8,9].

On a regular basis, cells employ multiple types of DNA repair mechanisms: base excision repair (BER), nucleic acid excision repair, homologous recombination (HR), single strand annealing (SSA), mismatch repair, and nonhomologous end joining (NHEJ) [10]. These mechanisms are favorable for normal cells to recover from injuries, but not in case of cancer therapy, where the goal is to kill the tumor cells through causing DNA damage in response to cytotoxic agents or radiation [11]. Recently, inhibition of specific enzymes involved in DNA repair mechanisms, poly (ADP-ribose)

* Corresponding authors at: Institute of Oncology Ljubljana, Department of Experimental Oncology, Zaloska 2, SI-1000 Ljubljana, Slovenia.

E-mail addresses: mbosnjak@onko-i.si (M. Bosnjak), tjesenko@onko-i.si (T. Jesenko), bmarkelc@onko-i.si (B. Markelc), larisa.janzic@mf.uni-lj.si (L. Janzic), mcemazar@onko-i.si (M. Cemazar), gsersa@onko-i.si (G. Sersa).

polymerase (PARP) enzymes, has become extensively researched due to the favorable activity reported in triple negative breast cancer and *BRCA* 1/2 mutated ovarian or breast cancer [12,13]. PARP enzymes are a family of 18 proteins responsible for catalyzing the reaction of adding the ADP-ribose to targeted proteins such as histones, topoisomerases, DNA helicases or some other proteins bound to the DNA molecule [14]. PARP1 and 2 are required to repair single strand breaks (SSBs). PARP1 is also involved in the repair of DNA double strand breaks (DSBs) and is present in the replication forks [15]. PARP 1 and PARP 2 are critical for the function of BER, but are involved also in other types of DNA repair mechanisms [16]. *BRCA* deficient cells were found to be much more sensitive to PARP inhibition than wild type cells [17], since *BRCA*1 and *BRCA*2 are also proteins involved in DNA break repair, more specifically required for HR [18,19]. Therefore, since *BRCA*-mutated cells are incapable of HR, which is considered as the most precise DSB repair mechanism, additional PARP inhibition results in genomic instability, cell arrest in G2 or M phases of the cell cycle and finally cell death [14,20,21]. PARP inhibitors in combination with cytotoxic therapy has already been studied. DNA methylating agents, including dacarbazine and temozolomide cause SSBs that in combination with PARP inhibitors could not be repaired [22].

As electroporation is a physical method for drug delivery, the entry of drugs in ECT can be effective for different cell lines and tumors. However, different effectiveness was reported in different histological types of tumors. It is most effective in basal cell carcinoma (85% CR), followed by melanoma while (64%) in breast cancer it has lower effectiveness (50–62% CR) [4,23,24]. Therefore, there is a need to increase the effectiveness of ECT in less responsive tumor types.

In our preliminary study, we combined ECT with bleomycin or cisplatin with PARP inhibitor olaparib in estrogen positive breast cancer cell line MCF7, without *BRCA* mutation, to test the feasibility and effectiveness of the combined approach [25]. The rationale behind the combined treatment is that olaparib would prevent the repair of DNA damage caused by ECT with bleomycin or cisplatin, thus potentiating its effectiveness. We demonstrated that olaparib potentiated the cytotoxic effect of ECT with bleomycin but not cisplatin in MCF7 cells [25].

The aim of our current study was to investigate the effect of olaparib in combination with ECT in *BRCA*1 mutated and non-mutated triple negative breast cancer cells, since *BRCA* mutation status determines the effectiveness of the DNA break repair. The effect of olaparib on the repair of therapy induced DNA damage was determined by staining of γ H2AX foci. The effectiveness of combined therapy was further studied in 2D and 3D cell cultures and *in vivo* in subcutaneous HCC1937 tumor model in immunodeficient SCID mice.

2. Materials and methods

2.1. Cell lines and drugs

Basal-like triple negative human breast cancer cell lines HCC1937 (ATCC[®] CRL-2336[™], *BRCA*1 mutated) and HCC1143 (ATCC[®] CRL-2321[™], *BRCA*1 non-mutated) were purchased from American Type Culture Collection (ATCC, Manassas, VA, USA) in 2018 and cultured in RPMI medium (Gibco, Thermo Fisher Scientific, Waltham, MA, USA) in a 5% CO₂ humidified atmosphere at 37 °C. Human breast cancer cells, luminal type A, estrogen receptor positive, progesterone receptor negative and HER2 negative, *BRCA* 1 non-mutated MCF7 (ATCC[®] HTB-22[™]) were also obtained from ATCC and cultured in advanced minimum essential medium (AMEM, Gibco). All cell media were supplemented with fetal bovine serum (FBS, Gibco), GlutaMAX (100x, Gibco), Penicillin-

Streptomycin (100x, Sigma-Aldrich, Merck, Darmstadt, Germany). The cells were routinely tested for mycoplasma infection by MycoAlert[™] PLUS Mycoplasma Detection Kit (Lonza, Basel, Switzerland) and were mycoplasma free.

A stock solution of 3 mg/ml bleomycin (Bleomycin medac, Medac, Germany) was diluted in 0.9% NaCl saline (B. Braun Melsungen AG, Melsungen, Germany) to 4 working solutions for HCC1143: 1.413, 0.706, 0.353 and 0.141 μ M and to 4 working solutions for HCC1937 cells: 0.141, 0.071, 0.014 and 0.007 μ M. Cisplatin Kabi 1 mg/mL (Fresenius Kabi, Bad Homburg, Germany) was diluted in 0.9% NaCl saline to 4 working solutions: 166.66, 16.67, 1.67, 0.17 μ M. Olaparib (10 mM, Selleckchem, Houston, TX, USA) was diluted in 0.9% NaCl saline to 5 working solution: 100, 50, 10, 5 and 1 μ M.

2.2. Electrochemotherapy *in vitro*

Monolayer of 80% confluent cells was trypsinized, centrifuged and resuspended in electroporation buffer (250 mM sucrose; 10 mM K₂HPO₄; 2.5 mM KH₂PO₄; 2 mM MgCl₂·6H₂O). A cell suspension of 2.2 × 10⁷ cells/ml was prepared. For each experimental group 10⁶ cells in 40 μ L were mixed with 10 μ L of bleomycin, cisplatin (CDDP) or in case of controls 10 μ L of saline. Concentration of CDDP and bleomycin were thus additionally diluted for 5 times. 50 μ L of the resulting mixture was pipetted between two electrodes (2 mm gap) and electroporated (8 pulses, 1300 V/cm, 100 μ s duration at frequency 1 Hz) with an Electro Cell B10 electric pulse generator (LEROY Biotech, Saint-Orens-de-Gameville, France). Five minutes after ECT, medium was added and cells were seeded for further assays. For viability assay 2 × 10³ HCC1937 and HCC1143 cells of each experimental group were plated in 0.1 ml of pertinent media in 96-well plate and incubated at 37 °C in a 5% CO₂ humidified incubator for 72 h.

2.3. Olaparib treatment

Cell were prepared as previously described and 2 × 10³ HCC1937 and HCC1143 cells were plated in 90 μ L of pertinent media in 96-well plate. Olaparib, which is highly permeable drug, was added to the cells (10 μ L) in different working concentrations (100, 50, 10, 5 and 1 μ M) and incubated for 72 h. Then, the cell survival assay was performed.

2.4. Cell survival assay

Cell survival was measured with Presto Blue viability assay (Thermo Fisher Scientific) 72 h after ECT or addition of olaparib. Presto Blue (10 μ L/well) was added to the cells and 30 min thereafter fluorescence intensity was measured by microplate reader (Infinite 200, Tecan, Männedorf, Switzerland). The viability of the cells was normalized to control untreated group. Based on this results effective dose of each cytotoxic drug, which kills half of cell population (EC₅₀), was determined.

2.5. Combined therapy of ECT and olaparib

Further combination experiments with combined therapy were performed with EC₅₀ dose of ECT with bleomycin or CDDP. Again, 2 × 10³ HCC1937 and HCC1143 cells were plated in 90 μ L of pertinent media in 96-well plate after ECT. Two hours after ECT treatment, when the cells attached, in half of the wells of each experimental group 10 μ L of selected olaparib dose (5 μ M) was added and in the other half of wells 10 μ L of NaCl saline. After 72 h, cell survival was determined as described above. The combined effects (additivity, synergism, and antagonism) of the treatments with independent mechanisms was determined. Additive

effect occurs when the combined effect of two drugs is equal to the sum of the effect of each drug given alone. When the effect of two drugs is greater than the sum of the effects of each drug given alone, the effect is called synergistic. This was calculated according to following formulas [26]:

$$Q = \ln(\bar{x}_1) + \ln(\bar{x}_2) - \ln(\bar{x}_{1+2}) - \ln(\bar{x}_{control}) \quad (1)$$

$$SE = \sqrt{\frac{\left(\frac{\sigma_1}{\bar{x}_1}\right) + \left(\frac{\sigma_2}{\bar{x}_2}\right) + \left(\frac{\sigma_{1+2}}{\bar{x}_{1+2}}\right) + \left(\frac{\sigma_{control}}{\bar{x}_{control}}\right)}{n_1 + n_2 + n_{1+2} + n_{control}}} \quad (2)$$

Where \bar{x}_1 = average, n = number of samples, σ = SD, x_1 = ECT, x_2 = olaparib, x_{1+2} = ECT + olaparib.

The results of both formulas provides an information about the combined affect: $Q < -2SE$ antagonism, $-2SE < Q < 2SE$ additivity and $Q > 2SE$ synergism.

2.6. Immunofluorescent staining of γ H2AX *in vitro*

To elucidate the mechanism of action of combined therapy, the histone H2AX, which in response to DNA double strand breaks (DSBs) rapidly phosphorylates to γ H2AX, was stained.

One day before staining, 5×10^3 HCC1937 and HCC1143 or 20×10^3 MCF7 cells were seeded on ibidi 12 well chamber slides (ibidi GmbH, Gräfelfing, Germany). Next day, ECT was performed on the attached cells. A 200 μ L of EP buffer or combination of EC₅₀ dose bleomycin or CDDP and EP buffer was pipetted into each well of the ibidi slide. Custom made plate electrodes for the electroporation of attached cells in ibidi slides (6.45 mm gap) were used for electroporation with same parameters as described above in chapter 2.2. Five minutes after ECT, EP buffer was replaced with pertinent media and 5 μ M olaparib was added thereafter and incubated at 37 °C. First, we optimized the time points with the maximal presence of γ H2AX foci (data not shown). The staining was performed on cells fixed in 4% paraformaldehyde (PFA; Alfa Aesar, MA, USA) for 15 min at 37 °C two hours after ECT. Further, the plasma membrane was stained with 1 μ g/ml WGA AlexaFluor 647 conjugate solution (Thermo Fisher Scientific) in Hanks' Balanced Salt Solution (HBSS, with calcium and magnesium, Gibco, Thermo Fisher Scientific) for 10 min at room temperature. Between these steps, the wells were washed twice with HBSS for 3 min. Cells were permeabilized with 0.1% Triton X-100 (Sigma-Aldrich) in phosphate-buffered saline (PBS) for 10 min at room temperature. Non-specific binding was blocked for 1 h in blocking buffer (5% donkey serum, 0.05% Tween 20, 22.52 mg/ml glycine in PBS). Cells were incubated overnight with anti- γ H2AX primary antibody (dilution 1:500, ab26350, Abcam, VB) in blocking solution (2% donkey serum, 0.05% Tween 20, 22.52 mg/ml glycine in PBS) at 4 °C. The next day, cells were washed twice with PBS for 3 min and incubated with Alexa Fluor 488 secondary antibody (dilution 1:500, ab150105, Abcam, Cambridge, UK) in blocking solution (2% donkey serum, 0.05% Tween 20, 22.52 mg/ml glycine in PBS) for 1 h at room temperature. Cells were then washed twice with PBS for 3 min and nuclei were stained with 3 μ g/ml of Hoechst solution (Hoechst 33342, Trihydrochloride, Trihydrate, Thermo Fisher Scientific) in PBS for 15 min at room temperature. Cells were again washed twice with PBS, the silicon wells were removed, and the slides were mounted with a Prolong Gold Diamond Antifade Mount (Thermo Fisher Scientific). Imaging was performed with an LSM 800 confocal microscope (Carl Zeiss) with a 63x oil immersion objective (NA 1.4). Hoechst 33342, Alexa Fluor 488 and Alexa Fluor 647 were excited with lasers with excitation wavelengths of 405 nm, 488 nm and 640 nm, respectively. The emitted light was collected sequentially with Gallium Arsenide Phosphide (GaAsP) detector via a variable dichroic and filters at the following wave-

lengths: 410 – 545 nm (Hoechst 33342), 488 – 545 nm (Alexa Fluor 488), and 645 – 700 nm (Alexa Fluor 647). The collected images were then visualized in Imaris software (Bitplane, Zurich, Switzerland). The number of γ H2AX foci in nuclei was quantified with Imaris software (Bitplane).

2.7. Spheroids preparation

Effects of combined therapy on spheroids were performed only in HCC1937 and MCF7 cells, since in HCC1143 there was no additional effect after combining ECT with olaparib, *in vitro* in 2D cell cultures. Breast cancer cells were harvested, counted and plated (2×10^3 HCC1937 or 4×10^3 MCF7 cells) in each well of 96-well U-bottom plates (Corning Incorporated, Corning, NY, USA) in 150 μ L of media, and then the plates were centrifuged for 2 min at 1000 rcf. Thereafter cell media was supplemented with hydroxypropyl methylcellulose in a final concentration of 10% (METHO-CELTM E50 Premium LV Hypromellose, Dow Chemical Company, Midland, Michigan, USA). The spheroids were then incubated for 3 days in a 5% CO₂ humidified incubator at 37 °C until they reached approximately 400 μ m in diameter. On this day, ECT was performed as described below (2.8).

2.8. Combined therapy of ECT and olaparib on spheroids

Each spheroid was transferred from a 96 well plate to a sterile 10 cm Petri dish, as previously described [27]. The media around spheroid was removed and the spheroid was washed with electroporation buffer. Then, 40 μ L of EP buffer and 10 μ L of cytotoxic drug (or saline for the control) was added to each spheroid. Electrodes with 2 mm gap were placed around the spheroid and eight 1300 V/cm pulses of 100 μ s duration at frequency 1 Hz were applied. After 5 min, the spheroids were transferred to a new 96-well U-bottom plate in cell medium containing 10% hydroxypropyl methylcellulose for further analysis. In corresponding groups, olaparib was added in concentration of 5 μ M.

Immediately after the ECT (day 0), and on days 3, 5 and 7 images of the spheroids were captured with Cytation 1 (BioTek, Winooski, VT, USA) and spheroid area were determined by the Gen5 software. For each group, 4 spheroids in 3 different experiments were measured and average area was calculated. The area of each spheroid was first normalized to day 0, and then for each group, the average normalized area was calculated and plotted as a growth curve.

2.9. Animals, tumors and treatment protocol *in vivo*

Six weeks old female immunodeficient SCID mice (CB17/Icr-Prkdcscid/IcrIcoCr1) were purchased from Charles River Laboratories (Calco, Italy) and kept at room temperature with a 12-h light-dark cycle in a specific pathogen-free environment with food and water ad libitum. Triple negative, *BRCA1* mutated breast cancer tumors were induced by subcutaneous injection of 2×10^6 HCC1937 cells in 100 μ L of 0.9% NaCl saline. Tumor volume was measured using a Vernier caliper, and calculated with the equation for an ellipsoid: $V = \pi \times (a \times b \times c)/6$ (where a, b and c are three perpendicular diameters of the tumor). When the tumors reached 6 mm in the longest diameter (~ 40 mm³), the mice were divided randomly into experimental groups, consisting of 9 mice, and the treatment started according to the protocol below. The experiments were approved by the Ministry of Agriculture, Forestry and Food of the Republic of Slovenia (permit no. U34401-1/2015/7), and were in compliance with the EU directive.

First, the effectiveness of ECT with two different doses of bleomycin was determined. Selection of the standard bleomycin dose (5 mg/kg) for ECT was based on previous studies [28,29] and was

in the range where complete responses of different tumor models were expected. Further, we also selected 50% reduced dose of bleomycin (2.5 mg/kg) for combination studies, a dose that is alone not causing complete tumor eradication and is appropriate for studying combined mechanisms of action. The experimental groups were: Control (no treatment), EP (electric pulses-only), i.v. bleomycin 5 mg/kg (retro-orbital injection of appropriate volume of 1,375 µg/ml bleomycin dissolved in 0.9% NaCl), i.v. bleomycin 2.5 mg/kg (retro-orbital injection of appropriate volume of 687.5 µg/ml bleomycin dissolved in 0.9% NaCl), ECT i.v. bleomycin 5 mg/kg and ECT i.v. bleomycin 2.5 mg/kg (retro-orbital injection of bleomycin following by ECT).

For ECT, bleomycin (5 or 2.5 mg/kg) was injected intravenously (i.v.) and after 3 min, tumors were treated with eight 1300 V/cm electrical pulses of 100 µs duration at 1 Hz. The electric pulses were delivered by ELECTRO Cell B10 electric pulse generator (Leroy Biotech) using 2 stainless steel plate electrodes with 6-mm gap in between.

The olaparib dose was also selected and diluted based on previous publications [30,31]. Before combination study, 5 mice were administered with selected intraperitoneal (i.p.) single dose (50 mg/kg) of olaparib and observed for next 48 h to access safety and feasibility of the procedure.

For combined therapy, mice were first i.p. administered olaparib and after half hour, when the concentration of olaparib in the tumors was expected to be maximal [31], bleomycin was administered i.v. For combined therapy, only the bleomycin dose 2.5 mg/kg was used, and pulses were again delivered 3 min after i.v. injection.

The animal body weight and well-being (changes in behavior, coat and skin condition) were monitored during the experiment as the indicator of systemic toxicity of the therapy. When the tumors reached 350 mm³, the mice were sacrificed and survival (Kaplan-Meier) curves were drawn.

2.10. Tumor histology on paraffin sections

Tumors were excised at three different time points after the therapy; 4, 24 and 72 h after the therapy. Half of the tumor was fixed in formalin (BD Pharmingen, BD Biosciences, San Jose, CA, USA) overnight and embedded in paraffin. Consecutive 2-µm thick tumor sections were cut from each paraffin block. The first section was stained with hematoxylin and eosin (H&E) to estimate the percent of necrotic tumor area. Second, proliferative area was stained with antibodies against Ki-67 (clone SP6, Thermo Fisher Scientific) at a dilution of 1:1000. The primary antibodies were detected with a peroxidase-conjugated streptavidin-biotin secondary antibody (Rabbit specific HRP/DAB detection IHC kit, ab64261, Abcam) according to manufacturer instructions. The images of stained tumor sections were captured with a DP72 CCD camera connected to a BX-51 microscope (Olympus, Hamburg, Germany). Whole tumor sections were captured with a 4x and 10x objective for H&E staining and 5 images with a 60x objective of the Ki-67 staining. Two independent observers determined the percentage of tumor necrosis and the percent of Ki-67 positive cells.

2.11. Tumor and spheroid immunofluorescence on frozen sections

The other half of the tumor and spheroids, processed 2 h after the treatment, were first fixed in 4% paraformaldehyde (PFA; Alfa Aesar) overnight, then incubated in 30% sucrose for 24 h, embedded in Optimal cutting temperature compound (OCT compound) and snap frozen in liquid nitrogen. Then, 14-µm thick tumor and 20-µm spheroid sections were cut using Leica CM1850 cryostat, dried for 30 min at 37 °C and washed for 5 min in 1X PBS. Antigen retrieval was performed by putting the slides into a hot 10 mM

sodium citrate buffer with 0.05% Tween 20 (approx. 95 °C) which was cooled down on air, at room temperature for 30 min followed by 30 min cooling in room temperature water. After the washing in PBS, the sections were blocked/permeabilized in blocking buffer with 0.5% Tween 20 for 30 min at RT in a humidified chamber. Further, sections were blocked for 1 h at RT in blocking buffer (5% donkey serum, 22.52 mg/ml glycine in PBS), and afterwards incubated with primary antibodies γH2AX (dilution 1:200, ab26350, Abcam) for tumors and spheroids and CD31 (dilution 1:200, AF3628, R&D systems, MN, US) for tumors overnight in blocking buffer (2% donkey serum, 22.52 mg/ml glycine in PBS) in a humidified chamber at 4 °C. After washing in PBS, sections were incubated with secondary antibodies (Alexa Fluor 488 (dilution 1:500, ab150105, Abcam), Alexa Fluor 647 (dilution 1:500, 705-605-147 Jackson ImmunoResearch, UK) in blocking buffer (2% donkey serum, 22.52 mg/ml glycine in PBS) for 1 h at RT in a humidified chamber and then washed in PBS. Nuclei were counter stained with Hoechst solution (3 µg/ml) in PBS for 10 min in the dark. After another wash in PBS, slides were mounted with ProLong™ Glass Antifade Mountant (Thermo Fisher Scientific). Imaging was performed with an LSM 800 confocal microscope (Carl Zeiss) with a 20x objective (NA 0.8). Hoechst 33342, Alexa Fluor 488 and Alexa Fluor 647 were excited with lasers with excitation wavelengths of 405 nm, 488 nm and 640 nm, respectively. The emitted light was collected sequentially with Gallium Arsenide Phosphide (GaAsP) detector via a variable dichroic and filters at the following wavelengths: 410 – 545 nm (Hoechst 33342), 488 – 545 nm (Alexa Fluor 488), and 645 – 700 nm (Alexa Fluor 647). Two 4x4 tile-scans were acquired for each tumor or 2x2 tile-scans for each spheroid. The collected images were then visualized and quantified in Imaris software (Bitplane).

2.12. Statistical analysis

The values in this study are represent as arithmetic mean (AM) ± standard error of the mean (SE) unless otherwise stated. The data were first tested for normality of distribution with the Shapiro-Wilk test. Comparison between two groups was performed using unpaired 2-tailed Student's *t*-test. The comparison of means of multiple was evaluated by one-way ANOVA followed by a Dunnett's multiple comparisons test. *P*-value of less than 0.05 was considered to be statistically significant. GraphPad Prism (GraphPad, San Diego, CA, USA) was used for statistical analysis and graphical representation. The log-rank (Mantel-Cox) test was performed on the Kaplan-Meier estimates.

3. Results

3.1. Sensitivity of cells to ECT or treatment with olaparib

Two different triple negative breast cancer cell lines, one with *BRCA1* mutation (HCC1937) and the other one without it (HCC1143) showed different sensitivity to ECT with bleomycin or CDDP (Fig. 1). *BRCA1* mutated cell line HCC1937 proved to be 10 times more sensitive to ECT with bleomycin than the HCC1143 cell line that does not have *BRCA1* mutation; EC₅₀ doses were 0.014 µM for HCC1937 (Fig. 1A) and 0.141 µM for HCC1143 (Fig. 1B). No significant difference in EC₅₀ was observed for ECT with CDDP between the two cell lines; EC₅₀ doses were 16.67 µM for HCC1937 (Fig. 1C) and 50 µM for HCC1143 (Fig. 1D).

Sensitivity of both triple negative breast cancer cell lines to olaparib was also tested. As expected, *BRCA1* mutated cell line HCC1937 (Fig. 1E) was more sensitive to olaparib treatment compared to non-mutated HCC1143 (Fig. 1F). For further combination experiments 5 µM olaparib was selected based on our previous

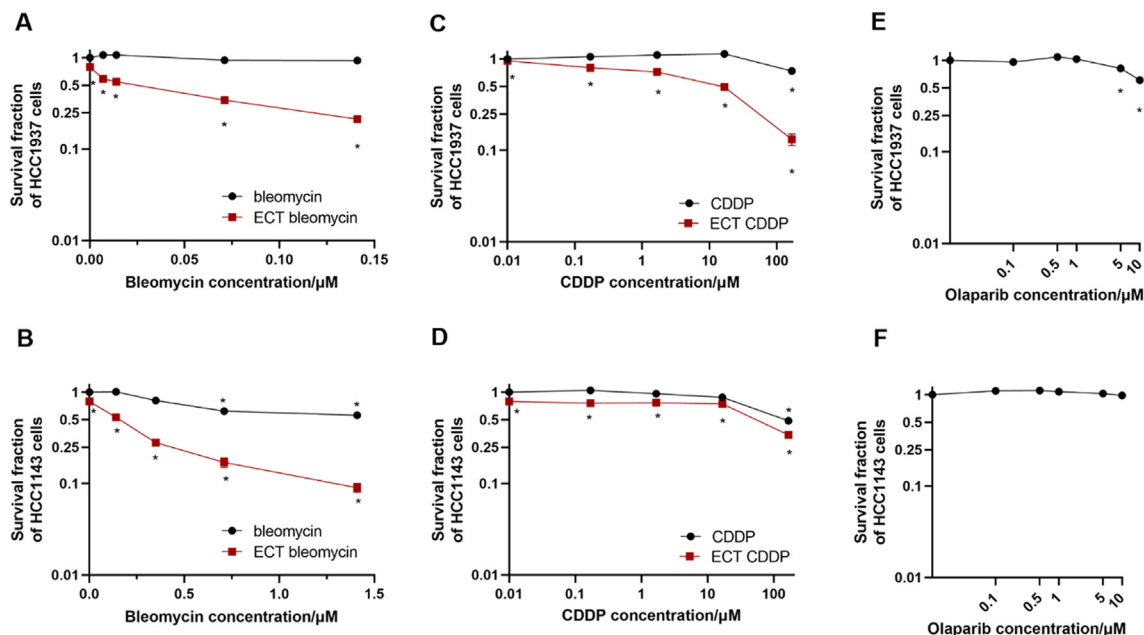


Fig. 1. Survival of breast cancer cell lines after ECT or olaparib treatment. Survival of HCC1937 (A) and HCC1143 (B) cells after ECT with bleomycin and survival of HCC1937 (C) and HCC1143 (D) cells after ECT with CDDP (log × axis) 72 h after the treatment. Survival after olaparib treatment for HCC1937 (E) and HCC1143 (F) was also determined 72 h after the treatment. The values are presented as the AM ± SEM. *p < 0.05 statistically significant difference compared to untreated control cells.

experiments and literature data [32]. At this concentration, no reduction in cell survival was observed for HCC1143 cell line. Contrary, approximately 20% reduction in cell survival was observed for HCC1937 cell line.

3.2. Olaparib increased the effectiveness of ECT in BRCA1 mutated cells

In the combined treatment experiments, EC₅₀ doses of ECT with bleomycin or CDDP were used, as determined in previous experiments (Fig. 1, 3.1). Olaparib was added to the ECT treated cells after they adhered to the surface of 96 well plate in the concentration of 5 μM. Between the two different triple negative cell lines, significant differences in potentiation of ECT with olaparib were observed. In the BRCA1 mutated HCC1937 cell line, olaparib significantly potentiated the effectiveness of ECT either with bleomycin (Fig. 2A) or CDDP (Fig. 2B) (p < 0.05). The interaction between the treatments was calculated. In case of ECT with bleomycin and olaparib the effect of two drugs given together was greater than the sum of the effects of each drug given alone. Calculated Q was 0.18 and calculated 2SE was 0.15, which means that Q > 2SE, which indicates on synergistic effect. In the case of ECT with CDDP and olaparib calculated Q was 0.01 and calculated 2SE was 0.12, which means that -2SE < Q < 2SE, which indicates on additive effect. On the contrary, no potentiation of ECT effectiveness either with bleomycin or CDDP was observed in the BRCA1 non-mutated HCC1143 cell line (Fig. 2C, 2D). Sensitivity of HCC1937 cells was also increased by olaparib treatment when cells were treated with electric pulses, bleomycin or CDDP only (Fig. 2A, 2B). No such effect was observed in the HCC1143 cells.

3.3. Combined therapy induces increased number of DNA double strand breaks in ECT with bleomycin

In our preliminary study, we demonstrated that olaparib potentiates the effectiveness of ECT with bleomycin in the estrogen receptor positive MCF7 human breast cancer cell line, but the underlying mechanism of action has not been determined yet [25]. For this purpose, we explored whether olaparib increases the number of DNA

strand breaks after ECT and for this reason γH2AX foci were stained in MCF7, HCC1937 and HCC1143 breast cancer cell lines.

When cells were treated with ECT with EC₅₀ dose of bleomycin a different extent of DNA damage was observed 2 h after the treatment (Fig. 3). In the MCF7 and HCC1937 cells several γH2AX foci (green dots) were observed, as well as approximately 15% of cells with entirely degraded DNA (entirely green nuclei) (Fig. 3 A,B). In the HCC1143 cells, almost all cells that were positive for γH2AX antibody presented with nuclei with entirely degraded DNA (Fig. 3C). When ECT with EC₅₀ dose of bleomycin was combined with olaparib, a significant difference was observed in the MCF7 and HCC1937 cells, with increased number of γH2AX foci per cell and increased number of cells with entirely degraded DNA, the percent of such cells was approximately 70%. Contrary, no significant difference was observed in the HCC1143 cells.

Differently, when cells were treated with ECT with EC₅₀ dose of CDDP, there was no statistically significant change in the number of γH2AX foci (green dots) per cells in any of the three tested cell lines. Moreover, when ECT with EC₅₀ dose of CDDP was combined with olaparib, no significant difference was observed in any of the three tested cell lines 2 h after the treatment (Fig. 3).

Interestingly, when HCC1937 cells were treated with pulses only (EP) combined with olaparib, a trend in increase of γH2AX foci was observed, however non-significant. This finding correlates with significantly decreased cell survival of HCC1937 after EP combined with olaparib, shown in Fig. 2B. Since this cell line is BRCA1 mutated it seems that is more prone for DNA damage, already after EP. This DNA damage could be corrected by the cells, but not (or hardly) in the presence of PARP inhibitor olaparib.

3.4. Effects of ECT in combination with olaparib on 3D cell cultures - spheroids.

Further, we investigated the effects of combined treatment on 3D cell culture, spheroids, as there 3D structure and organization more closely mimics tumors *in vivo* than 2D cell cultures. Here, only the MCF7 and HCC1937 cells were studied, since in HCC1143 there was no additional effect after combining ECT with olaparib (Fig. 2C,

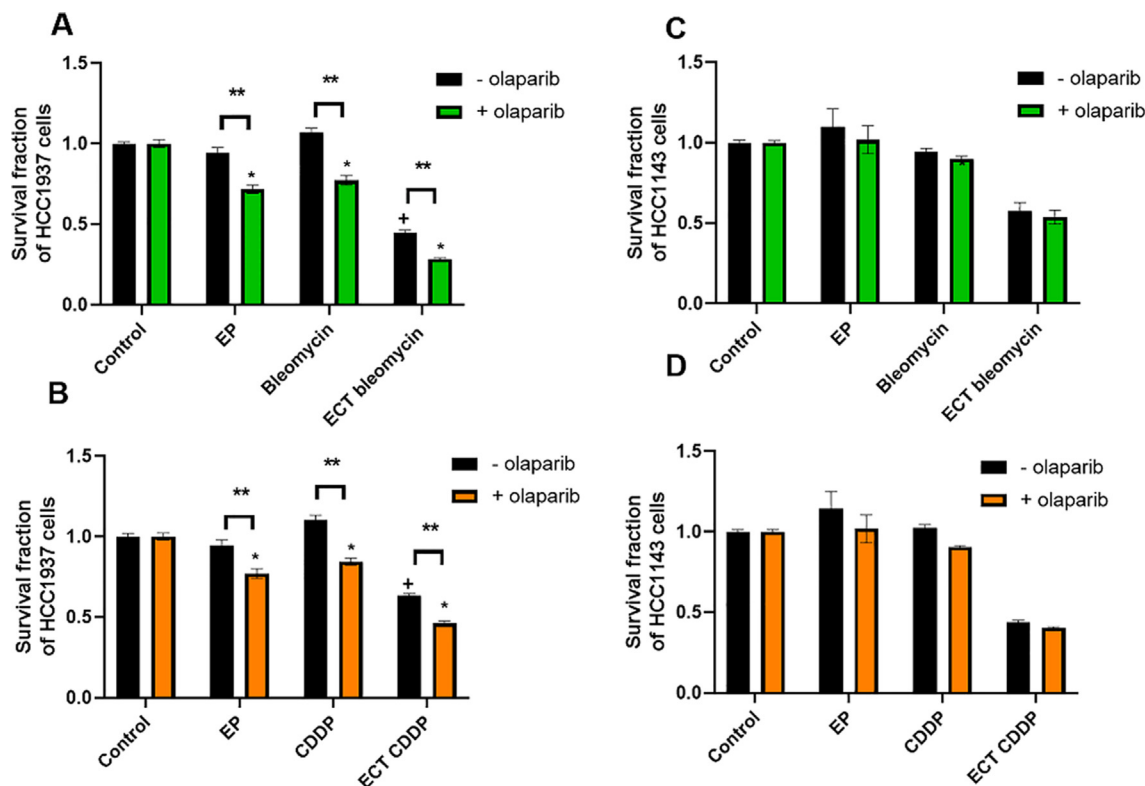


Fig. 2. Survival of breast cancer cell lines after combination of ECT and olaparib. Survival of HCC1937 cells after ECT with bleomycin and olaparib (A) or with CDDP and olaparib (B) and survival of HCC1143 cells after ECT with bleomycin and olaparib (C) or with CDDP and olaparib (D) 72 h after the treatment. The values are presented as the AM \pm SEM. + $p < 0.05$ statistically significant difference compared to untreated control cells; * $p < 0.05$ statistically significant difference compared to control + olaparib; ** $p < 0.05$ statistically significant difference between indicated groups.

D). The growth of MCF7 spheroids was significantly reduced after ECT with bleomycin (0.706 μ M) and ECT with CDDP (16.67 μ M) (Fig. 4A, C). After the addition of olaparib the growth of spheroids was even more reduced, especially in the ECT bleomycin group (Fig. 4A), where the difference was significant. Contrary, the addition of olaparib to ECT CDDP did not significantly affect the growth of MCF7 spheroids (Fig. 4B, C).

Growth of HCC1937 spheroids was also significantly reduced after ECT with bleomycin and ECT with CDDP (Fig. 5A-C). After the addition of olaparib the growth of spheroids was further reduced in all experimental groups (Fig. 5A-C), with significant difference determined only when olaparib was combined with bleomycin and ECT compared to ECT with bleomycin alone (Fig. 5A). As was already observed in the MCF7 cell line, the addition of olaparib to ECT CDDP did not significantly affect the growth of HCC1937 spheroids (Fig. 5B).

We further stained HCC1937 spheroid sections for DNA double strand breaks (γ H2AX) to confirm *in vitro* findings and mimic *in vivo* conditions. Since no additional effect on spheroid growth was observed when combining ECT CDDP and olaparib (Fig. 5B) in HCC1937 spheroids, only experiments with bleomycin were performed. Significant increase in % of all γ H2AX positive and in % of highly γ H2AX positive cells per spheroid section was observed when ECT was combined with olaparib compared to ECT alone (Fig. 6). Significant increase in % of all γ H2AX positive cells and in % of highly γ H2AX positive cells per spheroid section, was observed when olaparib was added to all other groups (control, bleomycin and EP) compared to groups without olaparib. The majority of DNA damage was located in the periphery of spheroids, however when olaparib was added the DNA damage effect was observed more into the core of the spheroid and only the most central part of the spheroid stayed undamaged.

3.5. Effects of combined therapy *in vivo*

Since HCC1937 tumor cells and spheroids were very sensitive to ECT with bleomycin *in vitro*, we first tested the effectiveness of ECT with two different doses of *i.v.* administered bleomycin; 5 mg/kg and 2.5 mg/kg dose of bleomycin. ECT with both doses significantly delayed tumor growth and therefore also survival of mice (Kaplan-Meier estimate, $p = 0.0005$ for 5 mg/kg and $p = 0.0013$ for 2.5 mg/kg). There was also a significant difference in the survival between ECT with 5 mg/kg and 2.5 mg/kg doses of bleomycin in favor of the 5 mg/kg dose ($p = 0.0085$) (Fig. 7A).

Further, we investigated the combination with single ECT treatment and single olaparib treatment. The aim was to observe, if the combined therapy could prolong survival or even cause some complete tumor responses. Olaparib was administered *i.p.* 30 min before ECT in order to provide maximal intratumoral olaparib concentration at the time of ECT [31]. The bleomycin dose 2.5 mg/kg was selected for combination studies. Already a single *i.p.* injection of olaparib significantly prolonged the survival of treated mice ($p = 0.0238$) compared to the untreated mice (control group) (Fig. 7B). The combined therapy of ECT with bleomycin 2.5 mg/kg dose and olaparib also prolonged the survival of treated mice ($p = 0.0483$) in comparison to the mice treated with ECT 2.5 mg/kg dose of bleomycin only. However, no complete responses were observed after the combined therapy. Addition of olaparib to ECT with bleomycin in HCC1937 tumor model had only minimal effect, indicating repetitive olaparib treatment would be needed.

The combined therapy was well tolerated with no significant weight loss or observed signs of pain or discomfort.

To investigate the underlying mechanisms of action of the combined therapy *in vivo* we stained tumor sections with H&E to determine the presence of necrosis, with anti-Ki-67 antibody to

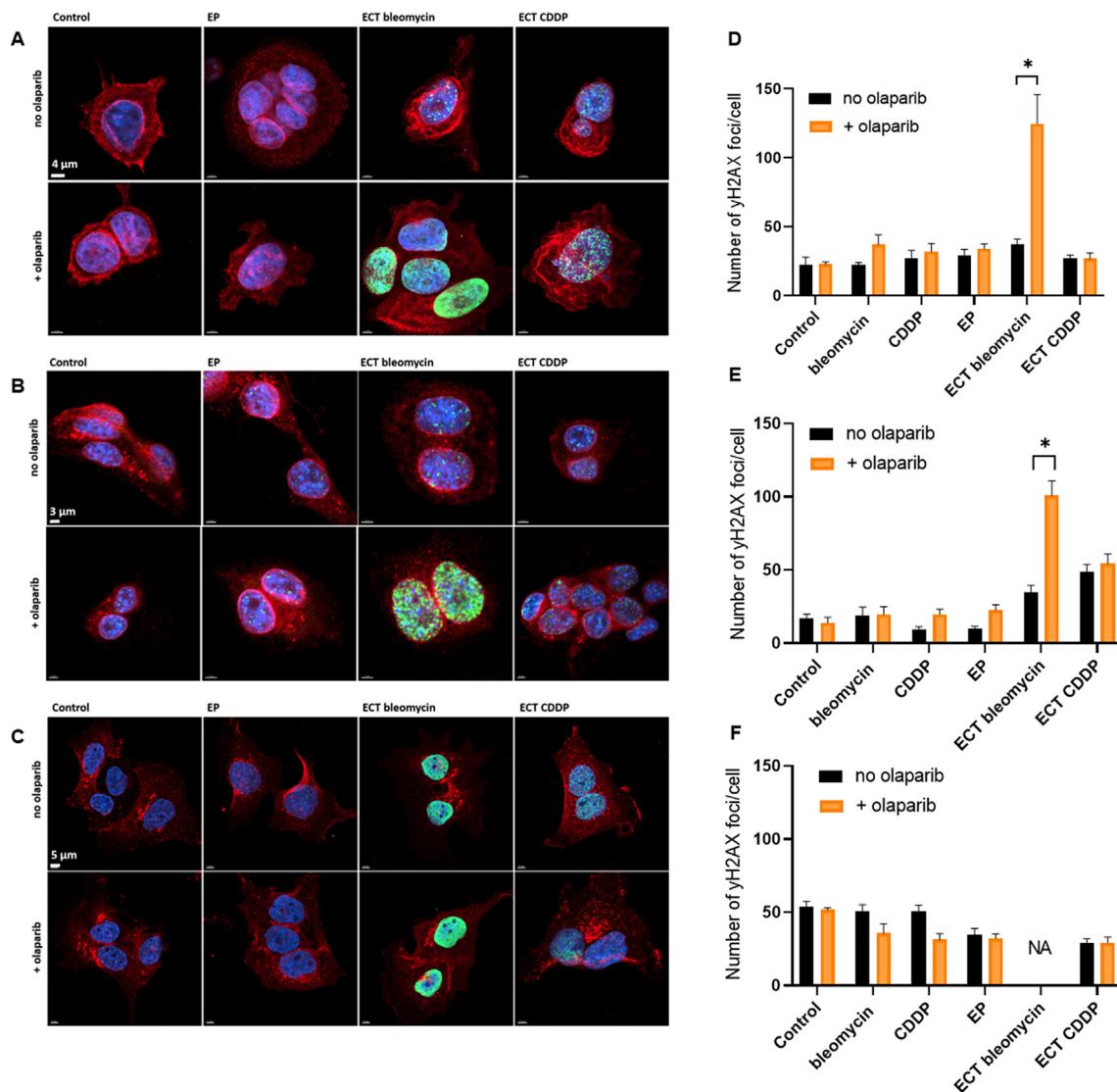


Fig. 3. DNA double strand breaks after the therapy. Representative images of γ H2AX histone staining of DNA double strand breaks in three different cell lines MCF7, (A), HCC1937 (B) and HCC1143 (C) was performed to determine the extent of the DNA double strand breaks. Blue-nucleus; red-plasma membrane, green- γ H2AX. Values on the graphs are presented as the AM \pm SEM. * $p < 0.05$ statistically significant difference between indicated groups. NA- not applicable for determination. Scale bar = 4 μ m (A), 3 μ m (B), 5 μ m (C).

determine the proliferative fraction of tumors and with anti- γ H2AX antibody to evaluate the extent of DNA double strand breaks throughout the tumor.

After ECT with bleomycin, there was a central necrotic part with a residual viable rim (Fig. 8). Tumors staining for Ki-67 showed reduced proliferative parts of tumors after the ECT (Fig. 8). The addition of olaparib further increased the extent of tumor necrosis and reduced the presence of Ki-67 positive proliferative areas. However, the difference in the necrotic area and the percent of the Ki-67 positive nuclei on the analyzed tumor sections was not significantly different between the ECT with bleomycin alone and the combination with olaparib (Fig. 8).

We also stained tumor sections for DNA double strand breaks (γ H2AX) and tumor vessels CD31 (Fig. 9). When combining ECT pulses and olaparib *in vivo* there was no difference in survival curves between pulses (EP) only or EP + olaparib. The same was true for combining bleomycin with olaparib (Supplementary image 1). Therefore, in accordance with 3R rule we did not planned for histology. Significant increase in the percent of γ H2AX positive

nuclei was observed at 4 and 24 h after the ECT treatment alone or in combination with olaparib compared to control tumors (Fig. 9A, B). However, there was no significant difference between ECT alone or in combination with olaparib. 72 h after the treatment the DNA damage was already repaired or the cells were dead. In the olaparib single treatment group the significant increase in the percent of γ H2AX positive nuclei was observed only after 4 h, but not after 24 h and 72 h. We also observed that some nuclei have a higher fluorescence intensity than others (Fig. 9A, C), indicating on the different extent of induced DNA damage and probably the ability of the cells to repair such breaks. These nuclei with high fluorescent intensity were almost solely observed in the tumors where ECT with bleomycin or the combination with olaparib was performed. The percent of these highly γ H2AX positive was also statistically increased in a similar manner as the overall percent of γ H2AX positive nuclei (Fig. 9C). We also observed that in the parts of tumors, which were better vascularized, more γ H2AX positive nuclei were observed compared to the parts of tumors, where vascularization was poor (Fig. 9A). This indicates

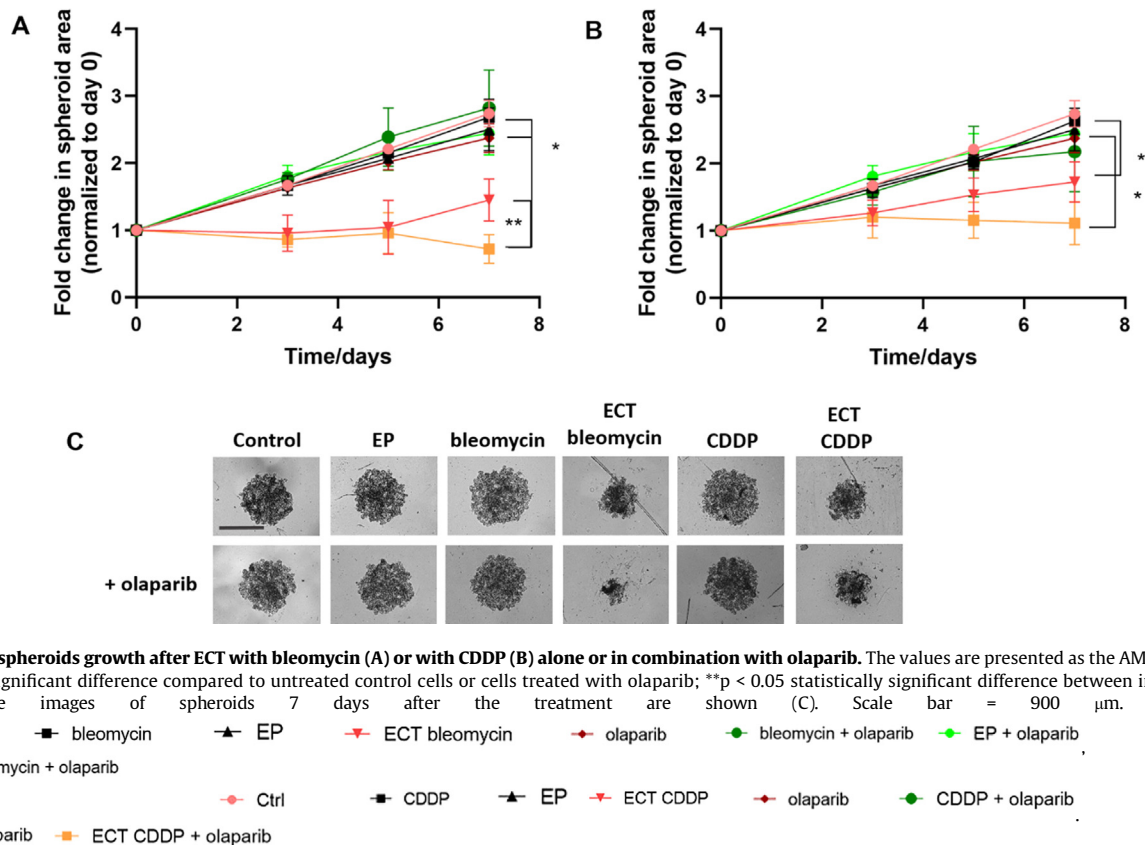


Fig. 4. MCF7 spheroids growth after ECT with bleomycin (A) or with CDDP (B) alone or in combination with olaparib. The values are presented as the AM ± SEM. *p < 0.05 statistically significant difference compared to untreated control cells or cells treated with olaparib; **p < 0.05 statistically significant difference between indicated groups. Representative images of spheroids 7 days after the treatment are shown (C). Scale bar = 900 μm. Legend: (A)

(B)

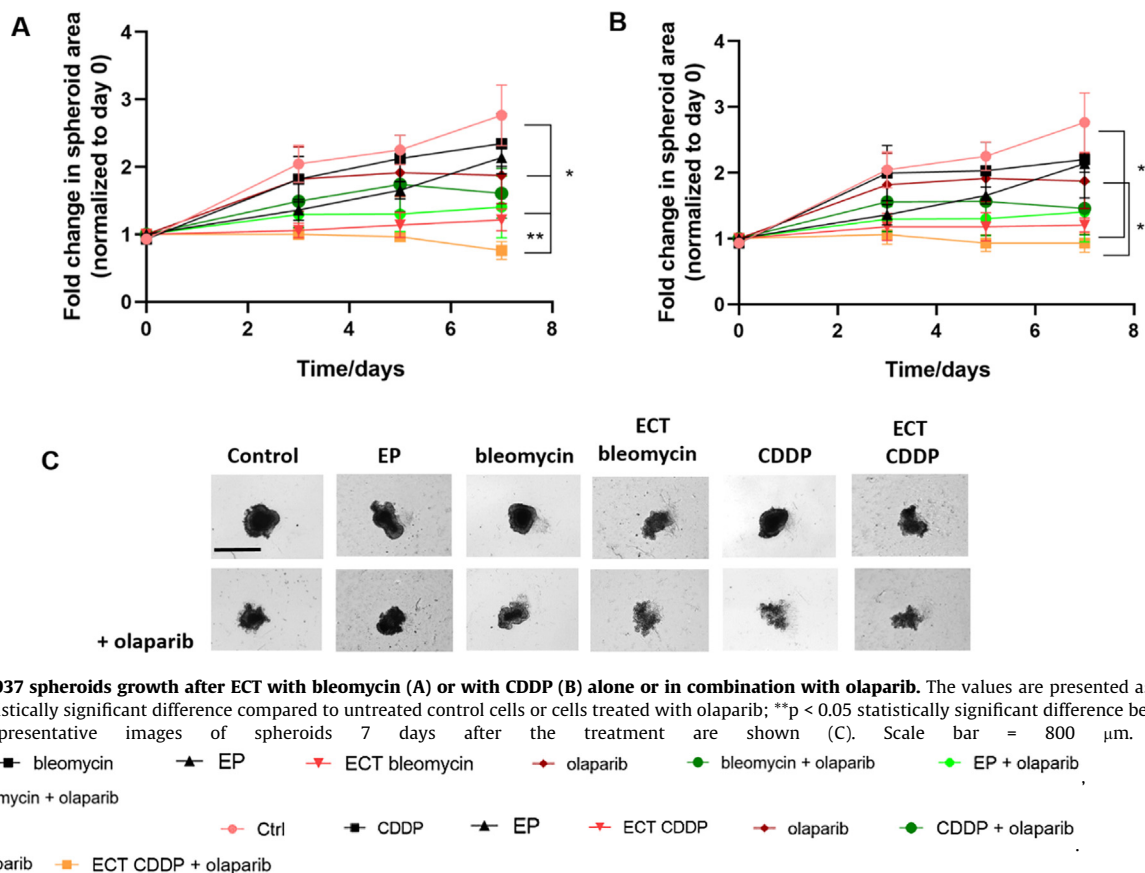


Fig. 5. HCC1937 spheroids growth after ECT with bleomycin (A) or with CDDP (B) alone or in combination with olaparib. The values are presented as the AM ± SEM. *p < 0.05 statistically significant difference compared to untreated control cells or cells treated with olaparib; **p < 0.05 statistically significant difference between indicated groups. Representative images of spheroids 7 days after the treatment are shown (C). Scale bar = 800 μm. Legend: (A)

(B)

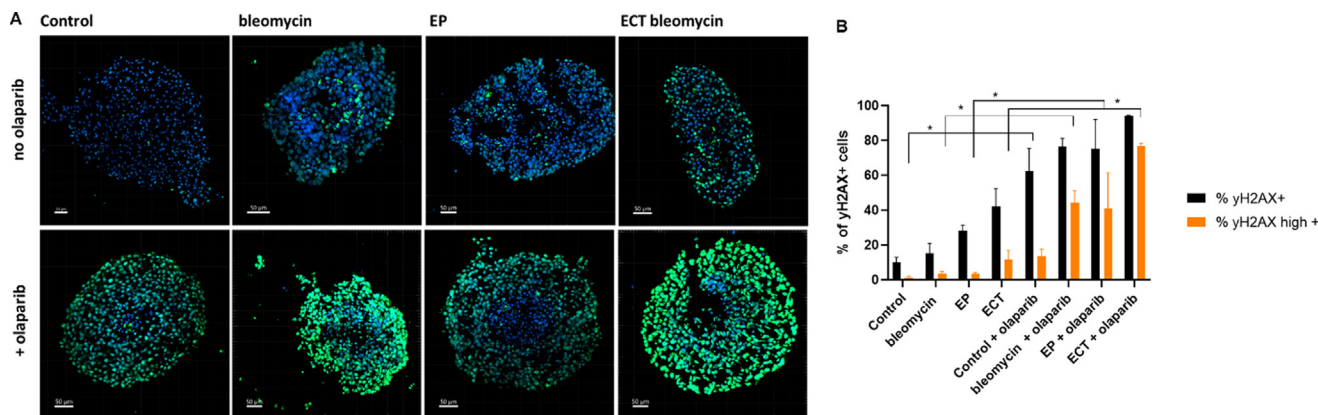


Fig. 6. Spheroid section stained for DNA double strand breaks (γ H2AX). Representative images of γ H2AX stained DNA double strand breaks; γ H2AX- green, nucleus - blue (A) and percent (%) of all γ H2AX positive and % of highly γ H2AX positive cells per spheroid section (B). Values on the graph are presented as the AM \pm SEM. * $p < 0.05$ statistically significant difference between indicated groups. Scale bar: 50 μ m.

that tumor vascularization is important for the distribution of bleomycin and olaparib and plays an important role in determining the effectiveness of ECT with bleomycin and the combined therapy.

4. Discussion

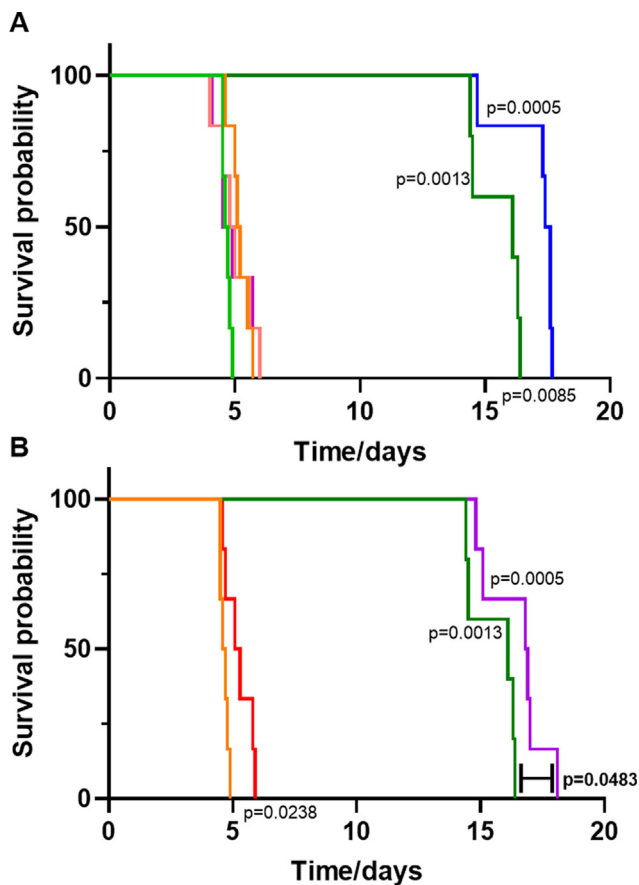
In this study, we demonstrated that ECT with bleomycin or cisplatin in triple negative breast cancer cell lines, with different *BRCA1* mutation status have different effectiveness alone or in combination with olaparib. The *BRCA1* mutation proved to be important for the sensitivity of ECT with bleomycin, but not for

ECT with CDDP. PARP inhibitor olaparib thus potentiated the effectiveness of ECT with bleomycin only in *BRCA1* mutated triple negative breast cancer.

Furthermore, compared to our previous study it seem that hormone status of the cells also plays an important role in the response to ECT [25]. As also demonstrated in the literature our study demonstrated that estrogen receptor positive cell line was more sensitive to the combination than the triple negative cell line without *BRCA1* mutation [25,33]. Similar results were observed in a study, when cells were treated with different anticancer drugs such as docetaxel, vinorelbin, paclitaxel and others. MCF7 cells were more sensitive to all cytotoxic drugs in that study than the triple negative cell line MDA-MB-231 [33]. Another study, where tamoxifen was combined with hypericin photodynamic therapy, demonstrated that MCF7 cells were more sensitive to the combined therapy than MDA-MB-231 cells *in vitro* and *in vivo* [34]. Triple negative breast cancer cells have been shown to be more resistant to different types of cytotoxic therapies [35]. Also in the clinical settings, estrogen receptor positive breast cancers are known to be more susceptible to different therapies than triple negative breast cancers [36].

The intrinsic *in vitro* sensitivity to ECT with bleomycin or cisplatin was different for *BRCA1* mutated and non-mutated triple negative cell line. *BRCA1* mutated cells were much more sensitive to ECT with bleomycin, where the EC_{50} was 10 times lower than in the *BRCA1* non-mutated triple negative breast cancer cells. EC_{50} was lower also for ECT with CDDP, but only for three times. However, as observed also in our previous study the *in vitro* sensitivity did not correlate with the *in vivo* sensitivity to ECT with bleomycin [29]. Similar as in murine melanoma tumors B16F10, which were very sensitive to ECT with bleomycin *in vitro*, ECT with 5 mg/kg *in vivo* delayed tumor growth, but no complete tumor regressions were observed. In comparison to the other tumor model (TS/A) used in the same study where cells were less sensitive to ECT with bleomycin *in vitro*, but the *in vivo* response was significantly better, resulting in tumor growth delay and complete tumor regressions after using the same bleomycin dose for ECT [29]. Thus, we once more demonstrated that *in vitro* tumor cell sensitivity is not a predictive factor for *in vivo* tumor response to ECT with bleomycin.

As it was already observed in several *in vitro* studies, not only bleomycin and CDDP alone, but also ECT with bleomycin or CDDP is causing DNA damage, resulting in DNA double strand breaks [28,37,38]. Similarly, a recent study published by Gibot et al. showed increased number of γ H2AX foci after ECT with bleomycin or cisplatin, in human colorectal tumor cell line and primary



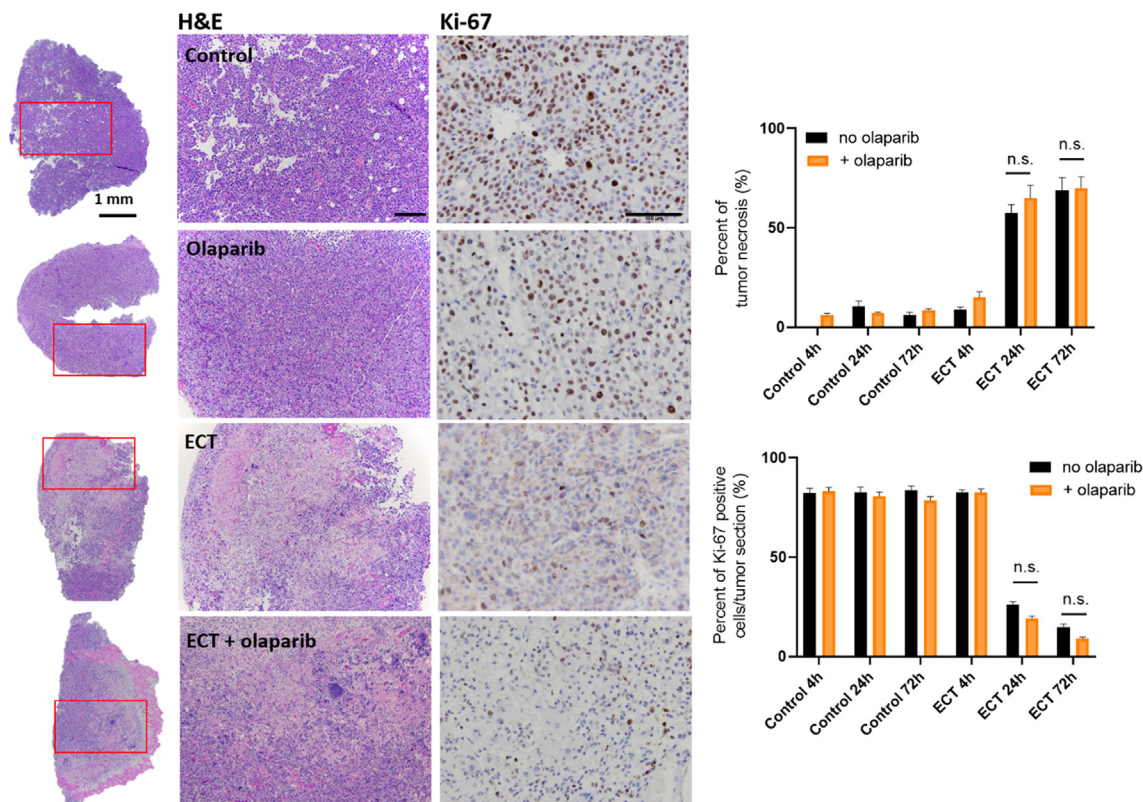


Fig. 8. Tumor necrosis (H&E) and proliferative parts (Ki-67 positive nuclei) after ECT with bleomycin alone or in combination with olaparib. Tumor necrosis and residual proliferative parts percentage over time are shown on the right side of the image. Although both of the features were significantly increased after 24 and 72 h, no significant difference was observed after ECT with bleomycin with or without olaparib. Scale bars: 200 μ m for H&E and 100 μ m for Ki-67.

fibroblasts [39]. We showed that after the addition of olaparib the extent of DNA damage was significantly increased after ECT with bleomycin in *BRCA1* mutated triple negative breast cancer cell line and spheroids (HCC1937) and also in the estrogen receptor positive cell line (MCF7), but not in the *BRCA1* non-mutated triple negative breast cancer cell line (HCC1143). In this way, we elucidated the mechanism of combined ECT bleomycin and olaparib treatment. The combined effects (additivity, synergism, and antagonism) of the treatments with independent mechanisms was determined [26]. We demonstrated that there is a synergism when ECT with bleomycin is combined with olaparib for the treatment of *BRCA1* triple negative (HCC1937) or estrogen receptor positive (MCF7) breast cancer cells. The results obtained with the staining of γ H2AX foci after combined ECT bleomycin and olaparib treatment correlated with the cell viability assay. Contrary, the increase in γ H2AX number was not significant when ECT CDDP was combined with olaparib. In the MCF7 cell line this was again in correlation with our previous study, where no additional reduction in cell survival was observed [25]. Differently, in the HCC1937 cells, cell survival after 72 h was reduced after addition of olaparib in ECT CDDP treatment group, even though we did not observe significant increase in the induced number of γ H2AX foci. The difference is

probably due to different mechanisms of action of the two cytotoxic drugs used for ECT; bleomycin is causing an immediate DNA damage by cleaving the DNA double strand and causing immediate extensive DNA double strand breaks. Whereas CDDP is causing DNA intra- and-interstrand adducts which have a delayed effect on the induced DNA damage at the time point when the cells are trying to replicate, but the replication forks are stalled due to CDDP. Therefore, we believe that additional, longer time points for staining the γ H2AX foci would better resolve the underlying mechanism in ECT CDDP and olaparib combination in HCC1937 cells. In a study in cervical cancer cell lines the increased number of γ H2AX foci was observed 24 h after combining olaparib with CDDP for 24 h [40].

When γ H2AX foci were stained *in vivo* on frozen tumor sections, we observed, that blood vessels had an important effect on the distribution of γ H2AX positive nuclei inside the tumor. The better-vascularized tumor areas had more γ H2AX positive nuclei than tumor areas located further from blood vessels. This indicates on non-equal distribution of bleomycin throughout the tumor. A similar observation was already reported in our previous study, where we demonstrated in *in vivo* murine tumor models that a predictive factor for tumor response to ECT with bleomycin is tumor vascular-

Fig. 7. Survival curves of HCC1937 tumor bearing SCID mice after ECT alone (A) or in combination with i.p. olaparib (B). Significant p values are presented between two groups or in the case of ECT bleomycin 5 mg/kg or 2.5 mg/kg or ECT bleomycin 2.5 mg/kg + olaparib compared to control, untreated group. Legend: (A)
 (B)

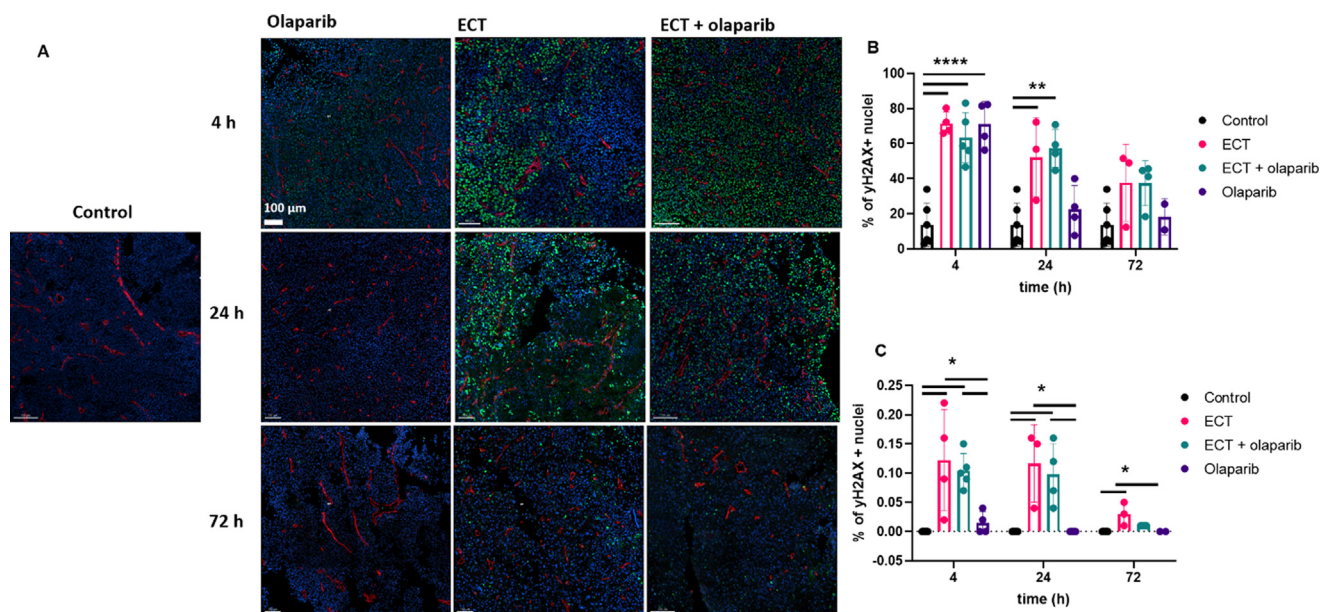


Fig. 9. Tumor section stained for DNA double strand breaks (γ H2AX). Representative images of γ H2AX stained DNA double strand breaks; γ H2AX- green, vessels (CD31) - red, nucleus - blue (A). Percent (%) of all γ H2AX positive nuclei per tumor section after the treatment (B) and % of highly γ H2AX positive nuclei per tumor section after the treatment (C). * $p < 0.05$ statistically significant difference between indicated groups; ** $p < 0.01$ statistically significant difference between indicated groups; **** $p < 0.001$ statistically significant difference between indicated groups. Scale bar: 100 μ m.

ization [29] and not the amount of cytotoxic drug in the tumor. One of the options for increasing the effectiveness of ECT with bleomycin and olaparib in HCC1937 tumor model would be to repeat the olaparib therapy for several consecutive days thus achieving a more homogenous distribution of olaparib in the tumor.

Similar as in our study PARP inhibitors have previously shown their potential to enhance the effects of DNA-damaging anticancer drugs such as temozolomide, platinum and cyclophosphamides in *BRCA1* deficient breast and ovarian cell lines [41]. In this study, we observed that adding olaparib to ECT with bleomycin *in vivo* had only moderate effect, indicating repetitive olaparib treatment would be needed. Similar was observed in other study of olaparib alone in *BRCA1* deficient mammary tumor model suggest that continuous i.p. dosing of 50 mg/kg olaparib (100 consecutive days) may be more effective than intermittent treatment (28 consecutive days) [31].

In recent clinical reports of breast cancer metastasis treated with ECT with bleomycin, low complete response rate was observed [4,24]. In the study of Matthiessen *et al.*, where effectiveness of ECT with bleomycin was evaluated only in breast cancer patients, the patients with different receptor status were included, i.e. estrogen, progesterone and HER2 receptor, as well as patients with triple-negative breast cancer. Unfortunately the analysis comparing the effectiveness between tumor subtypes was not performed [4]. A case report describing ECT with bleomycin in chest wall recurrence of *BRCA2* triple-negative breast showed partial necrosis of the tumor tissue and devascularization that reduced bleeding and serum production. Nevertheless, the local progression free survival was only about 30 days, improvement in pain management was observed [42]. We believe that such patients could benefit from the combined therapy. Our study indicates that hormonal and mutational status could influence the response rate in ECT treatment with bleomycin. In those cases where *BRCA1*, and presumably *BRCA2* as well, mutation is present, adjuvant olaparib treatment could enhanced ECT response. Furthermore, our data indicates that ECT could be safely applied in patients already receiving olaparib.

Drawback of the study is that only a single dose of olaparib, but not repetitive dosing, was used to investigate the combined therapy and underlying mechanisms. Although, our study is preliminary it warrants further studies with repetitive treatment of olaparib. The study was also performed only in one *BRCA1* mutated and one *BRCA1* non-mutated cell line, therefore, to generalize our findings, the combination of ECT and olaparib should be tested on several other breast cancer cell lines, including cell lines with known *BRCA2* mutation. Moreover, several other PARP inhibitors are currently under investigation or already in the clinical settings and would be an interesting alternative drugs for combination with ECT [43]. One of the drawback of the study is also that IC_{50} dose of bleomycin and CDDP were determined on cells in suspension, while γ H2AX quantification was performed on attached cells. Therefore more relevant would be to determine IC_{50} dose also for attached cells.

5. Conclusions

In this current study, we demonstrate that drugs that inhibit DNA repair, like olaparib, have the potential to increase ECT effectiveness with bleomycin. The synergistic effect was observed in *BRCA1* mutated breast cell line but not in *BRCA1* non-mutated. Addition of olaparib to ECT with bleomycin *in vivo* in HCC1937 tumor model had only minimal effect, indicating repetitive olaparib treatment would be needed. Further studies also on other cell lines and with other inhibitors are warranted.

Funding

This work was supported by the Slovenian Research Agency (ARRS), grant number Z3- 1871 and P3-0003.

Declaration of Competing Interest

The authors declare that they have no known competing financial interests or personal relationships that could have appeared to influence the work reported in this paper.

Acknowledgement

We would like to thank Mira Lavrič and Simona Kranjc Brezar for all the valuable help.

References

- [1] A. Marra, D. Trapani, G. Viale, C. Criscitiello, G. Curigliano, Practical classification of triple-negative breast cancer: intratumoral heterogeneity, mechanisms of drug resistance, and novel therapies, *Npj Breast Cancer* 6 (2020) 1–16, <https://doi.org/10.1038/s41523-020-00197-2>.
- [2] V. De Giorgi, M. Grazzini, B. Alfaioli, I. Savarese, S.A. Corciova, G. Guerriero, et al., Cutaneous manifestations of breast carcinoma, *Dermatol. Ther.* (2010), <https://doi.org/10.1111/j.1529-8019.2010.01365.x>.
- [3] C.L. Buchanan, P.L. Dorn, J. Fey, G. Giron, A. Naik, J. Mendez, et al., Locoregional Recurrence after Mastectomy: Incidence and Outcomes, *J. Am. Coll. Surg.* (2006), <https://doi.org/10.1016/j.jamcollsurg.2006.06.015>.
- [4] L.W. Matthiessen, M. Keshtgar, P. Curatolo, C. Kunte, E.M. Grischke, J. Odili, et al., Electrochemotherapy for Breast Cancer—Results From the INSPECT Database, *Clin. Breast Cancer* (2018), <https://doi.org/10.1016/j.clbc.2018.03.007>.
- [5] L.G. Campana, I. Edhemovic, D. Soden, A.M. Perrone, M. Scarpa, L. Campanacci, et al., Electrochemotherapy - Emerging applications technical advances, new indications, combined approaches, and multi-institutional collaboration, *Eur. J. Surg. Oncol.* 45 (2019) 92–102, <https://doi.org/10.1016/j.ejso.2018.11.023>.
- [6] L.G. Campana, D. Miklavčič, G. Bertino, R. Marconato, S. Valpione, I. Imarisio, et al., Electrochemotherapy of superficial tumors – Current status: Basic principles, operating procedures, shared indications, and emerging applications, *Semin. Oncol.* (2019), <https://doi.org/10.1053/j.seminoncol.2019.04.002>.
- [7] V. Murray, J.K. Chen, L.H. Chung, The interaction of the metallo-glycopeptide anti-tumour drug bleomycin with DNA, *Int. J. Mol. Sci.* 19 (2018), <https://doi.org/10.3390/ijms19051372>.
- [8] M. Enoiu, J. Jiricny, O.D. Schärer, Repair of cisplatin-induced DNA interstrand crosslinks by a replication-independent pathway involving transcription-coupled repair and translesion synthesis, *Nucleic Acids Res.* 40 (2012) 8953–8964, <https://doi.org/10.1093/nar/gks670>.
- [9] T. Makovec, Cisplatin and beyond: Molecular mechanisms of action and drug resistance development in cancer chemotherapy, *Radiol. Oncol.* (2019), <https://doi.org/10.2478/raon-2019-0018>.
- [10] P. Huertas, DNA resection in eukaryotes: Deciding how to fix the break, *Nat. Struct. Mol. Biol.* (2010), <https://doi.org/10.1038/nsmb.1710>.
- [11] S. Bhattacharya, A. Asaithamby, Repurposing DNA repair factors to eradicate tumor cells upon radiotherapy, *Transl. Cancer Res.*, 2017, <https://doi.org/10.21037/tcr.2017.05.22>.
- [12] P.C. Fong, D.S. Boss, T.A. Yap, A. Tutt, P. Wu, M. Mergui-Roelvink, et al., Inhibition of Poly(ADP-Ribose) Polymerase in Tumors from BRCA Mutation Carriers, *N. Engl. J. Med.* (2009), <https://doi.org/10.1056/NEJMoa0900212>.
- [13] J. O'Shaughnessy, C. Osborne, J. Pippen, M. Yoffe, D. Patt, G. Monaghan, et al., Efficacy of BSI-201, a poly (ADP-ribose) polymerase-1 (PARP1) inhibitor, in combination with gemcitabine/carboplatin (G/C) in patients with metastatic triple-negative breast cancer (TNBC): Results of a randomized phase II trial, *J. Clin. Oncol.*, 27 (2009) 3–3, https://doi.org/10.1200/jco.2009.27.18_suppl.3.
- [14] M. Rouleau, A. Patel, M.J. Hendzel, S.H. Kaufmann, G.G. Poirier, PARP inhibition: PARP1 and beyond, *Nat. Rev. Cancer* (2010), <https://doi.org/10.1038/nrc2812>.
- [15] Y. Pommier, M.J. O'Connor, J. De Bono, Laying a trap to kill cancer cells: PARP inhibitors and their mechanisms of action, *Sci. Transl. Med.* (2016), <https://doi.org/10.1126/scitranslmed.aaf9246>.
- [16] M. Wang, W. Wu, W. Wu, B. Rosidi, L. Zhang, H. Wang, et al., PARP-1 and Ku compete for repair of DNA double strand breaks by distinct NHEJ pathways, *Nucleic Acids Res.* (2006), <https://doi.org/10.1093/nar/gkl840>.
- [17] B. Evers, R. Drost, E. Schut, M. De Bruin, E. Van Burg, Derksen PWB Der, et al., Selective inhibition of BRCA2-deficient mammary tumor cell growth by AZD2281 and cisplatin, *Clin. Cancer Res.* (2008), <https://doi.org/10.1158/1078-0432.CCR-07-4953>.
- [18] J. Wu, L.Y. Lu, X. Yu, The role of BRCA1 in DNA damage response, *Protein Cell* 1 (2010) 117–123, <https://doi.org/10.1007/s12338-010-0010-5>.
- [19] Y. Liu, S.C. West, Distinct functions of BRCA1 and BRCA2 in double-strand break repair, *Breast Cancer Res.* 4 (2002) 9–13, <https://doi.org/10.1186/bcr417>.
- [20] H. Farmer, H. McCabe, C.J. Lord, A.H.J. Tutt, D.A. Johnson, T.B. Richardson, et al., Targeting the DNA repair defect in BRCA mutant cells as a therapeutic strategy, *Nature* (2005), <https://doi.org/10.1038/nature03445>.
- [21] M.K. Weil, A.P. Chen, PARP Inhibitor Treatment in Ovarian and Breast Cancer, *Curr. Probl. Cancer* (2011), <https://doi.org/10.1016/j.cuprobncancer.2010.12.002>.
- [22] L. Tentori, G. Graziani, Chemopotentiation by PARP inhibitors in cancer therapy, *Pharmacol. Res.* (2005), <https://doi.org/10.1016/j.phrs.2005.02.010>.
- [23] B. Mali, T. Jarm, M. Snoj, G. Sersa, D. Miklavčič, Antitumor effectiveness of electrochemotherapy: A systematic review and meta-analysis, *Eur. J. Surg. Oncol.* 39 (2013) 4–16, <https://doi.org/10.1016/j.ejso.2012.08.016>.
- [24] A.J.P. Clover, G. Bertino, P. Curatolo, J. Odili, L. Campana, C. Kunte, et al., Electrochemotherapy in the treatment of cutaneous malignancy; outcomes and subgroup analysis from the cumulative results from the pan-European INSPECT Database for 1478 lesions in 691 patients (2008–2018), *Eur. J. Surg. Oncol.* (2019), <https://doi.org/10.1016/j.ejso.2018.10.090>.
- [25] M. Bosnjak, L. Janzic, M. Cemazar, G. Sersa, Combining Electrochemotherapy with Targeted Therapy Olaparib in vitro, *Springer, Cham* (2021) 247–253, https://doi.org/10.1007/978-3-030-64610-3_29.
- [26] S.A. Spector, M. Tyndall, E. Kelley, Effects of acyclovir combined with other antiviral agents on human cytomegalovirus, *Am. J. Med.* 73 (1982) 36–39, [https://doi.org/10.1016/0002-9343\(82\)90060-2](https://doi.org/10.1016/0002-9343(82)90060-2).
- [27] K. Znidar, M. Bosnjak, T. Jesenko, L.C. Heller, M. Cemazar, Upregulation of DNA sensors in B16.F10 melanoma spheroid cells after electrotransfer of pDNA, *Technol. Cancer Res. Treat.* (2018), <https://doi.org/10.1177/1533033818780088>.
- [28] M.N. Zakelj, A. Prevc, S. Kranjc, M. Cemazar, V. Todorovic, M. Savarin, et al., Electrochemotherapy of radioresistant head and neck squamous cell carcinoma cells and tumor xenografts, *Oncol. Rep.* (2019), <https://doi.org/10.3892/or.2019.6960>.
- [29] A. Groseelj, S. Kranjc, M. Bosnjak, M. Krzan, T. Kosjek, A. Prevc, et al., Vascularization of the tumours affects the pharmacokinetics of bleomycin and the effectiveness of electrochemotherapy, *Basic Clin. Pharmacol. Toxicol.* (2018), <https://doi.org/10.1111/bcpt.13012>.
- [30] L. Henneman, M.H. Van Miltenburg, E.M. Michalak, T.M. Braumuller, J.E. Jaspers, A.P. Drenth, et al., Selective resistance to the PARP inhibitor olaparib in a mouse model for BRCA1-deficient metastatic breast cancer, *Proc. Natl. Acad. Sci. USA* (2015), <https://doi.org/10.1073/pnas.1500223112>.
- [31] S. Rottenberg, J.E. Jaspers, A. Kersbergen, E. Van Der Burg, A.O.H. Nygren, S.A.L. Zander, et al., High sensitivity of BRCA1-deficient mammary tumors to the PARP inhibitor AZD2281 alone and in combination with platinum drugs, *Proc. Natl. Acad. Sci. USA* (2008), <https://doi.org/10.1073/pnas.0806092105>.
- [32] E.C. Bourton, P.A. Ahorner, P.N. Plowman, S.A. Zahir, H. Al-Ali, C.N. Parris, The PARP-1 inhibitor Olaparib suppresses BRCA1 protein levels, increases apoptosis and causes radiation hypersensitivity in BRCA1+/- lymphoblastoid cells, *J. Cancer* 8 (2017) 4048–4056, <https://doi.org/10.7150/jca.21338>.
- [33] A.L. Risinger, N.F. Dybdal-Hargreaves, S.L. Mooberry, Breast cancer cell lines exhibit differential sensitivities to microtubule-targeting drugs independent of doubling time, *Anticancer Res.* 35 (2015) 5845–5850.
- [34] T.A. Theodossiou, M. Ali, M. Grigalavicius, B. Grallert, P. Dillard, K.O. Schink, et al., Simultaneous defeat of MCF7 and MDA-MB-231 resistances by a hypericin PDT-tamoxifen hybrid therapy, *Npj Breast Cancer* (2019), <https://doi.org/10.1038/s41523-019-0108-8>.
- [35] S. Hurvitz, M. Mead, Triple-negative breast cancer: Advancements in characterization and treatment approach, *Curr. Opin. Obstet. Gynecol.* 28 (2016) 59–69, <https://doi.org/10.1097/GCO.0000000000000239>.
- [36] O. Gluz, C. Liedtke, N. Gottschalk, L. Pusztai, U. Nitz, N. Harbeck, Triple-negative breast cancer - Current status and future directions, *Ann. Oncol.* (2009), <https://doi.org/10.1093/annonc/mdp492>.
- [37] O. Tounekti, G. Pron, J. Belehradec, L.M. Mir, Bleomycin, an Apoptosis-mimetic Drug That Induces Two Types of Cell Death Depending on the Number of Molecules Internalized, *Cancer Res.* 53 (1993) 5462–5469, <https://doi.org/10.1158/0008-5472.CCR-93-0309>.
- [38] O. Tounekti, A. Kenani, N. Foray, S. Orłowski, L.M. Mir, The ratio of single-to double-strand DNA breaks and their absolute values determine cell death pathway, *Br. J. Cancer* (2001), <https://doi.org/10.1054/bjoc.2001.1786>.
- [39] L. Gibot, A. Montigny, H. Baaziz, I. Fourquaux, M. Audebert, M.P. Rols, Calcium delivery by electroporation induces in vitro cell death through mitochondrial dysfunction without DNA damages, *Cancers (Basel)* (2020), <https://doi.org/10.3390/cancers12020425>.
- [40] C.B. Prasad, S.B. Prasad, S.S. Yadav, L.K. Pandey, S. Singh, S. Pradhan, et al., Olaparib modulates DNA repair efficiency, sensitizes cervical cancer cells to cisplatin and exhibits anti-metastatic property, *Sci. Rep.* (2017), <https://doi.org/10.1038/s41598-017-13232-3>.
- [41] C.K. Donawho, Y. Luo, Y. Luo, T.D. Penning, J.L. Bauch, J.J. Bouska, et al., ABT-888, an orally active poly(ADP-ribose) polymerase inhibitor that potentiates DNA-damaging agents in preclinical tumor models, *Clin. Cancer Res.* (2007), <https://doi.org/10.1158/1078-0432.CCR-06-3039>.
- [42] M.K. Radica, N. Fabbri, G. Sant'Andrea, S. Bonazza, A. Stefanelli, P. Carcoforo, Use of electrochemotherapy in a voluminous chest wall recurrence of triple-negative breast cancer: case report, *AME Case Reports* (2020), <https://doi.org/10.21037/acr-20-54>.
- [43] M. Yi, B. Dong, S. Qin, Q. Chu, K. Wu, S. Luo, Advances and perspectives of PARP inhibitors, *Exp. Hematol. Oncol.* 8 (2019) 29, <https://doi.org/10.1186/s40164-019-0154-9>.